Materials and Design 197 (2021) 109278

Contents lists available at ScienceDirect

Materials and Design

journal homepage: www.elsevier.com/locate/matdes

Definition of analytical cleaning procedures for archaeological pottery from underwater environments: The case study of samples from Baia (Naples, South Italy)

Michela Ricca [a], Beatriz Cámara [b], Rafael Fort [b], Mónica Álvarez de Buergo [b], Luciana Randazzo [a], Barbara Davidde Petriaggi [d], Mauro Francesco La Russa [a,c,*]

[a] University of Calabria, Department of Biology, Ecology and Earth Science, 87036 Arcavacata di Rende, CS, Italy
[b] Geosciences Institute IGEO (CSIC-UCM), Doctor Severo Ochoa 7, 28040 Madrid, Spain
[c] Institute of Atmospheric Sciences and Climate, National Research Council (ISAC-CNR), Via Gobetti 101, 40129 Bologna, Italy
[d] Istituto Superiore per la Conservazione ed il Restauro, Via di San Michele, 25, 00153 Rome, Italy

HIGHLIGHTS

- Multi-analytical study by microscopic techniques, XRD analysis, cleaning tests, colorimetric and ultrasound measurements
- Characterization of archaeological materials, their structure, properties, alteration and degradation products
- Final recognition of the extent of decay due to biological growth, affecting the durability of pottery
- Evaluation of the effects of cleaning procedures
- The data improve knowledge about preservation of ceramics from underwater and allow to set-up a protocol for their cleaning

GRAPHICAL ABSTRACT

ARTICLE INFO

Article history:
Received 19 May 2020
Received in revised form 31 August 2020
Accepted 29 October 2020
Available online 30 October 2020

Keywords:
Biodeterioration
Cleaning
Pottery
Ultrasounds
Underwater archaeology

ABSTRACT

This work is focused on a multidisciplinary study of 13 pottery fragments collected in the submerged archaeological site of Baia (Naples, Italy). Founded by the Romans in the 1st century B.C., this archaeological area represents one of the greatest evidences of Roman architecture and it includes ancient ruins whose structures range from maritime villas and imperial buildings. Several diagnostic tests were carried out in order to characterize the archaeological materials, their structure and properties, as well as the alteration and degradation products. Degradation forms in seawater imply not only a variation in the physico-mechanical and chemical properties of the material but also an aesthetic damage, due to superficial deposits, which can lead to the illegibility of the artefacts. In this context, it is crucial to determine to what extent these decay factors, mainly attributable to biological growth, could affect the durability of pottery and what are the effects of cleaning procedures. The work offers further elements to obtain new insights into the underwater cultural heritage field and in the function of ceramic matter, especially related to several applications in technology and in the adoption of strategies for suitable conservation procedures.

* Corresponding author.
E-mail address: mlarussa@unical.it (M.F. La Russa).

https://doi.org/10.1016/j.matdes.2020.109278

1. Introduction

Archaeological materials coming from underwater environments are of great relevance in order to study technologies, origin and progressive evolution of ancient civilizations and for a better understanding of historic events [1–5]. Underwater sites are highly dynamic environments and undergo the influence of the marine system. In particular, as regards archaeological artefacts, it is well known that they are exposed to several processes, mechanisms and decay forms; some closely related to the intrinsic properties and nature of the materials, such as their mineralogy and texture (i.e. pores and micro-cracks), while others are affected by the surrounding environment (i.e. wave motion and power, currents, tides, salinity, temperature, sediments, biological activity, etc.) [6–8]. In particular, regarding biological activity, the hard-fouling species that settle on exposed surfaces (i.e. archaeological materials) play a key role in the decay process, by increasing the available area for settlement and a specific area for alteration processes such that epibiosis phenomena occur [9–11]. As time passes, this process leads to the deposition of calcium carbonate in the form of skeletons or shells, together with the sedimentation that consolidates the structure and drives the community to succession. In this context, artefacts may be uncovered beneath sediments, chemically altered or even destroyed under the severe conditions of the seabed or suffering the consequences of bio-colonization [12–17].

When artefacts are discovered in the sea and considered to be of significant archaeological or historical importance, archaeologists, conservation scientists and experts in the field are faced with two courses of action: conserving the finding out of the sea, in subaerial conditions (i.e. museums), after proper recovery, or preserving them in situ on the seabed. Generally, when the archaeological assets are rather small and the depth of the seabed from the water surface is moderate, they can be easily recovered and undergone to conservation and cleaning processes to be exhibited. Different is the discovery of vessel wrecks and sunken loads as a result of shipping accidents at high depths, where in situ conservation and musealization is preferred. Anyway, during archaeological surveys, excavations or fortuitous findings, it is important to know and establish what the end use of the artefacts will be, along with their preliminary state of preservation [18]. These aspects will determine the most suitable choice for a preliminary study to be carried out and the proper method for conserving the find. In particular, if the choice falls on the recovery on land and the artefacts are not promptly treated, they will be susceptible to rapid deterioration, resulting unusable both for diagnostic purposes as for display them in a museum.

The adopted approach is addressed to the musealization of objects from underwater archaeological sites and represents one of the main goals of this study. In fact, the preservation of underwater cultural heritage (UCH) is the basis of recommendations of the international convention issued in 2001 by UNESCO [19] and, as a matter of fact, not only aims to ensure and strengthen the protection of UCH, but supports a proper study, documentation and protection of underwater artefacts in order to create public awareness and knowledge of the UCH [17,20–25].

This paper focuses on the current and common applications of diagnostic investigation and cleaning procedures [22–24] on underwater archaeological pottery, paying attention on the changes they suffer as a result of the removal of surface deposits. This will ensure the proper management of the conservation procedures based on the properties of materials and degradation phenomena as well as the most suitable managing of such archaeological assets in terms of musealization, use and fruition. The underwater archaeological park of Baia (Bacoli - Naples, South Italy) (Fig. 1) was chosen as a case study for the present research [12,14,21,26,27], where several pottery fragments belonging to different archaeological artefacts were recovered; then a battery of tests and diagnostic investigations was carried out.

2. Materials & methods

Sampling of pottery fragments was performed with the assistance of archaeologists of the *Soprintendenza Speciale per i Beni Archeologici di Napoli e Pompei* who retrieved such artefacts in different areas of the submerged site (Fig. 1) during one of their underwater archaeological surveys. The selection criteria according to which the samples were chosen were primarily based on their state of conservation and the degradation forms observed with the naked eye. As a primary objective, the present work aims at experimenting a protocol for the preservation of ceramic materials from underwater, in order to support a proper museum display. Specifically, thirteen fragments were studied with different and complementary techniques; a list of analysed samples along with a brief macroscopic description is summarized in Table 1.

Diagnostic investigations of the selected thirteen archaeological pottery were carried out in three main stages: a) the mineralogical-petrographic characterization on representative fragments taken from the artefacts; b) the characterization of superficial damage and alteration forms by studying the interaction between the biological colonization and the archaeological materials, and c) the cleaning tests and petrophysical investigations in order to define appropriate cleaning methods with respect to the ceramic body. Specifically, the analytical techniques applied for a complete characterization of the samples [i.e. stage a) and b)] includes:

- Observations under a stereomicroscope (EMZ-5D, MEIJI EM), performed in order to preliminarily identify the biological communities and superficial damage.
- Polarising light optical microscopy (PLOM) on thin sections to: i) determine the petrographic and textural features of ceramic fragments ii) understand the alteration mechanisms and evaluate the extent of the decay. Observations were performed using a Zeiss AxioLab microscope equipped with a digital camera to capture images.
- X-ray powder diffraction analysis (XRPD) to identify the constituent mineralogical phases. Analyses were performed on a D8 Advance Bruker diffractometer with CuKα radiation, using the following operative conditions: step-size of 0.02°2θ, step time of 2 s/step and an analytical range of 3–65°. No preliminary treatment, for example removal of salts by desalination procedure (bath method), was performed in order to keep the sample as it was (undisturbed) after its recovering from sea. Small portions of each sample were powdered (hand grinding) to pass through a 325 mesh sieve (45 μm).

Later, considering that superficial deposits are the main degradation products identified on the archaeological surfaces, some chemical and mechanical cleaning methods have been tested for their removal [i.e. stage c)]. Specifically, cleaning procedures carried out focused on the use of:

- Soft and hard bristle brushes for removing less coherent deposits and a mechanical ablator (micro-motor) for the toughest encrustations. The latter was performed by using piezoelectric micro—motor device for accurate mechanical cleaning ultrasonic device (micromotor ART 6000 CTS) at frequencies between 9000 and 15,000 r.p.m.
- EDTA (Ethylenediaminetetraacetic acid) 5% in distilled water (50 g / 1000 ml) at pH 7 in cellulose pulp according to the procedure proposed by [7].

Besides, both before and after surface cleaning tests, some physical and petrophysical properties were measured, such as chromatic and ultrasonic velocity measurements in order to evaluate changes occurring in pottery properties after the removal of the superficial layers. The tools used are respectively:

- A Minolta CM-700D spectrophotometer supported by the Colour Data SpectraMagic TM NX CM-S100W software for the data processing.

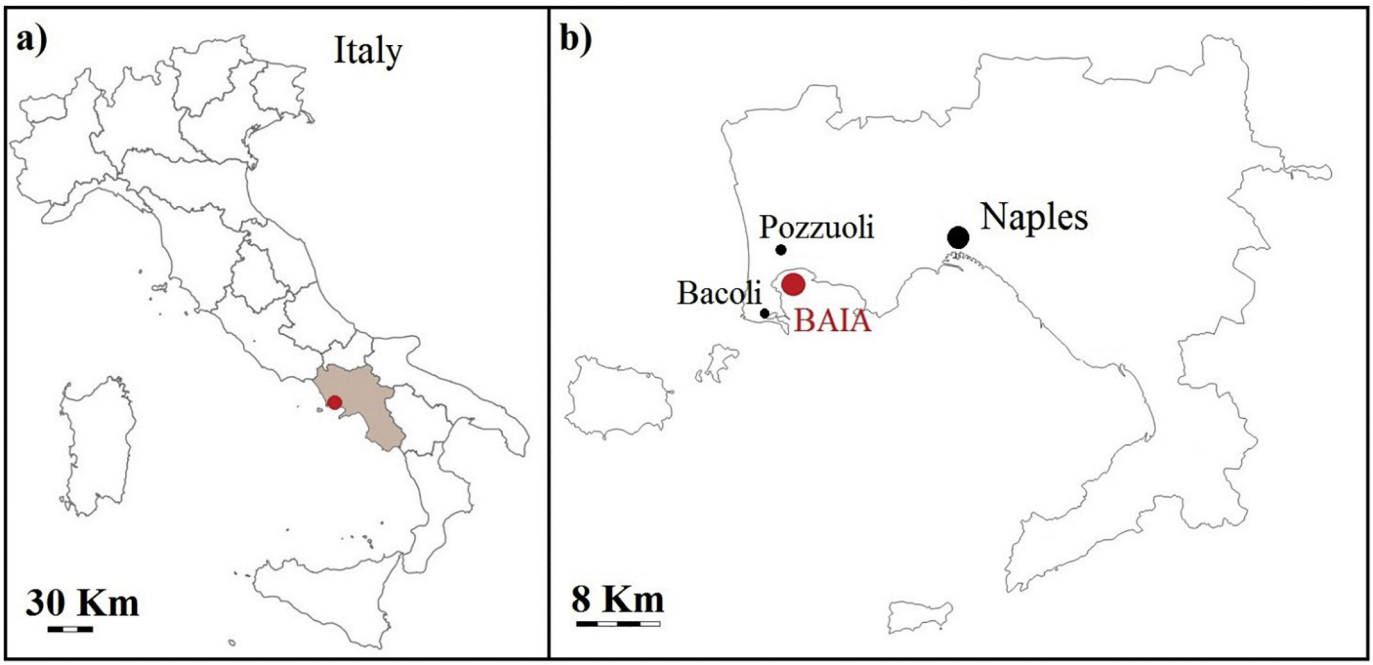

Fig. 1. Location of the underwater archaeological park of Baia in the Campanian region (a), province of Naples (b) – Italy.

This portable and non-destructive technique allowed to measure the changes in the ceramic materials chromatic parameters through the CIELab system, during cleaning procedures. Thanks to the lightness (L^*) and chromatic coordinates (a^* and b^*) values, the total colour change is then calculated by means of ΔE^*, following Italian recommendation [28].

- A non-destructive and portable Pundit CNS Electronics for ultrasound measurements. The technique allowed to measure the propagation speed of the ultrasound waves (P or longitudinal wave) through the samples, useful to evaluate and quantify the degree of deterioration of the archaeological artefacts [29–31] based on superficial encrustations, and determine whether the cleaning techniques produce variation in texture. In detail, measurements were made, distinguishing between the mechanical and chemical cleaning areas in each sample, according to: a) The direct method (transducers placed in parallel and opposite faces); b) indirect or surface method (both transducers on the same face) to determine the state in which the pieces studied were. For both methods, 1 MHz transducers of 0.8 mm in diameter were used in all cases. 6 measurements were recorded in direct method, per piece before cleaning. After cleaning, 3 measurements were made in each area selected for each type of cleaning (M: Mechanical and C: Chemical). Measurements were also carried out by indirect method. In this case it was 10 measurements on each piece (W) and 5 measurements for each area after mechanical and chemical cleaning. The distant between transducers was variable and depended on the irregularities of each sample.

3. Results and discussion

3.1. Stereomicroscopy

Observations under stereomicroscopy revealed some variability in the type and rate of biocolonization among the different examined items. Samples are diffusely covered by biological layers mainly made of encrusting bryozoans, calcareous algae, tubeworms, barnacles and other marine organisms which play key roles in the creation of complex biogenic structures, especially in the Mediterranean Sea [14,32]. Some samples show a slight biological growth characterized by thin superficial layers, while others exhibit a more abundant biological settlement where skeleton calcifications of different organisms prevail (i.e. samples C6, C7, C9 and C12 covered mostly by serpuloid worms, bryozoa and barnacles). A summary of the collected data is shown in Table 2 along with some representative images showing bio-colonization on samples surface (Fig. 2).

3.2. Polarising light optical microscopy (PLOM)

All the 13 sherds were subjected to thin sectioning for petrographic analysis. Samples belonged to several ceramic objects (Table 1) of both fine and coarse wares pottery. Petrographic analysis focused on the composition of fabrics characterizing the types, amounts, size ranges, roundness and sorting of non-plastic inclusions and types of accessory minerals. The microstructure of the clay matrices was also examined, such as the shape, orientation and size of voids, distribution of inclusions within the fabric. During observations, parameters were determined following the guidelines proposed by Whitbread [33]. The petrographic results are simplified for each of the ceramic sherds, highlighting their main features, which serve to link or separate them from each other; in fact, where similar, samples were described as a single group. Some representative photomicrographs are shown in Fig. 3, while Table 3 reports the main petrographic features detected for each sample.

Group 1 - Samples 1, 5, 9 & 12. Medium-Coarse grain (Type MC) (up to 2500 μm) pottery with heterogeneous and slightly porous groundmass, and quartz and rock fragment inclusions (mainly trachyte) (up to 5500 μm). Microstructure shows vugs and planar voids. Less abundant are vughy and slightly preferential oriented vesicles; their size varies between meso- and macro- and reach 2000 μm (2 mm) in diameter. The groundmass is characterized by high optical activity and brown-reddish colour in plane polar light (PPL). Only in C5, the groundmass colour varies from grey-brown in the core of the pot wall examined in thin section, to reddish-orange along the edges (PPL). The inclusions are mainly represented by monocrystalline quartz granules and rare policrystalline ones, followed by alkali feldspars, plagioclase, micas and iron oxides with size up to 2500 μm (2.5 mm). Also, pyroxene

Table 1
List of the examined archaeological pottery fragments taken from different areas within the submerged site.

Sample	Object	Fabric	Compactness	Photographic representation
C1	Fragment of coarse ware pottery	red-brown coarse fabric	medium	
C2	Fragment of fine ware pottery	Red fabric, fine-grained	medium	
C3	Neck-Amphora fragment	Grey-reddish fabric, fine-grained	medium	
C4	Fragment of pot's lid	Grey-reddish fabric, fine-grained	high	
C5	Fragment of pot's rim	Dark grey to reddish burnished fabric, coarse-grained	high	
C6	Fragment of ribbed amphora body	Orange fabric, fine-grained	medium	
C7	Neck-Amphora Fragment	Light brown to red burnished fabric, fine-grained	medium	
C8	Fragment of amphora stub	Orange fabric, fine-grained	medium	
C9	Fragment of amphora body	light beige to red fabric, medium to coarse grained	medium	
C10	Fragment of ribbed amphora body	white-beige fabric, fine-grained	high	
C11	Fragment of amphora handle	light beige to orange fabric, fine- grained	medium	
C12	Fragment of pot's rim	dark-brown fabric, medium to coarse grained	medium	
C13	Fragment of pot's rim	Grey-reddish fabric, fine-grained	medium	5 cm

Table 2
Summary of the collected data from the samples observed under a stereomicroscope, paying attention to superficial layers due to biocolonization and their main features.

Sample	Superficial layers description and damage
C1	Coherent and coarse deposit layer, brownish in colour alternating with lighter ones. It is mainly due to algal colonization, marine worms and bryozoans that almost cover the entire sample surface.
C2	Thin and coherent brownish patina that partially covers the surface. It is mainly due to algal colonization and sediments.
C3	Thin and coherent whitish patina that partially covers the surface. Mainly due to algal and bryozoan's colonization.
C4	Thin and coherent whitish patina that partially covers the surface. It is mainly due to algal colonization.
C5	Thin and coherent brownish patina that rarely covers the surface. It is mainly due to algal colonization and sediments.
C6	Coherent and rather coarse deposit layer, whitish in colour, due to zoobenthos colonization (i.e. serpuloid worms, bryozoa and barnacles).
C7	Coherent and rather coarse deposit layer ranging in colour from whitish to brownish due to serpuloid worms and bryozoa; also, green-brownish and whitish patina due to algae was detected.
C8	Sporadic serpuloid worms and slight adherent whitish patina that partially covers the sample's area, especially internally.
C9	Coherent and rather coarse deposit layer, yellow-whitish in colour, due to zoobenthos colonization (i.e. serpuloid worms and bryozoans). Brownish patina attributable to algal colonization.
C10	Thin and consistent patina, white to brownish, which covers almost all the sample surface due to serpulids, bryozoans and algae.
C11	Thin and consistent brownish patina which covers almost all the sample surface due to algae.
C12	Coherent and very coarse deposit layer, brownish in colour alternating with lighter and reddish ones. It is mainly due to barnacles and serpulids stratified colonizations, which almost cover the entire sample surface. Green-brownish patina due to algae and bryozoans was also observed.
C13	Thin and coherent brownish patina that partially covers the surface. It is mainly due to algal colonization and sediments.

only in C1 and C12 were detected. Fragments of rocks were also observed up to 5500 μm (5.5 mm), specifically volcanic (trachyte) in C1; metamorphic (quartzite) in C9, while both trachyte and quartzite along with cocciopesto (ceramic fragments) in C12. In sample C9, crystals' preferential orientations are also visible (Fig. 3c). Finally, amorphous concentration features (Acfs), mainly given by pure nodules and impregnant portions [29] commonly occur as discrete grains of opaque material in all the samples.

Group 2 - Samples 2, 6, 7, 8, 10, 11 & 13. Fine-grained (Type F) pottery (up to 750 μm) with a quite homogeneous groundmass, and quartz inclusions. The microstructure is characterized by vugs and vesicles, the latter ones show slightly preferential orientation with regular shape and smooth surface; their size falls into the meso-pores range, with diameters from 100 to 350 μm. The groundmass is characterized by a medium-low optical activity and dark-reddish colour in PPL. The inclusions are mainly fine and very fine-grained and characterized by dominant quartz, rounded and sub-rounded in shape, along with feldspar and iron-oxides. Also in C8, C10, C11 and C13 calcite and fossils (50–600 μm) are present. Fragments of metamorphic rocks are also present along with dark brown amorphous phases.

Group 3 - Samples 3 & 4. Medium-Fine grained (Type MF) pottery (up to 900 μm) with homogeneous groundmass, and quartz and rock fragment inclusions. The microstructure is characterized by vugs, vesicles and planar voids with size between 70 and 400 μm in diameter. Only sample 4 shows macro-pores with sizes up to 1100 μm. Secondary calcite along the boundary of the pores is also present. The groundmass shows a high optical activity with a brown-reddish colour in PPL. As inclusions, quartz, feldspars, plagioclase, pyroxene, amphiboles, micas, iron oxides and calcite (from 100 μm to 900 μm) along with fragments of metamorphic, volcanic and sedimentary rocks, specifically carbonatic, (from 200 μm to 1200 μm) were detected. Acfs [33], mainly given by pure nodules, was observed.

Besides, according to Whitbread [33], a semi-quantitative estimation of the coarse fraction/fine fraction/vughs (i.e. c/f/v ratio (%) or groundmass/aggregate/pore ratio) was carried out by a visual valuation for each sample (Table 3). Such semi-quantitative estimation varies from 60/35/5, 40/40/20, 45/40/15 for samples belonging to Group 1 (Type MC); from 45/40/15, 50/40/10, 45/50/5, 50/45/5 and 50/40/10 for the ceramics of the Group 3 (Type MF) and finally, it is of 45/40/15 for the two samples of the Group 2 (Type F). More details are in Table 3.

Observations by OM also highlighted how the distribution of the colonization is quite variable among the samples. Encrusting assemblages made of stratified deposition of calcium carbonate in the form of skeletons, especially related to algae, bryozoa and barnacle's activity, are

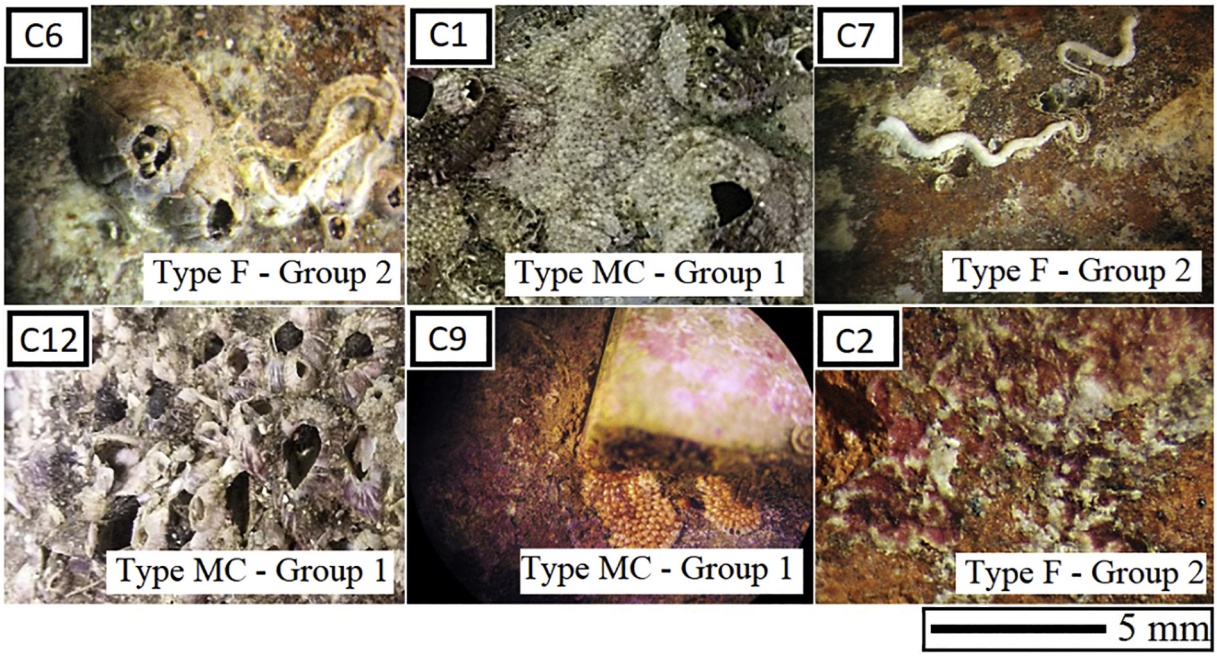

Fig. 2. Representative photomicrographs of samples C6, C1, C7, C12, C9 and C2 showing biocolonization as reported in Table 2.

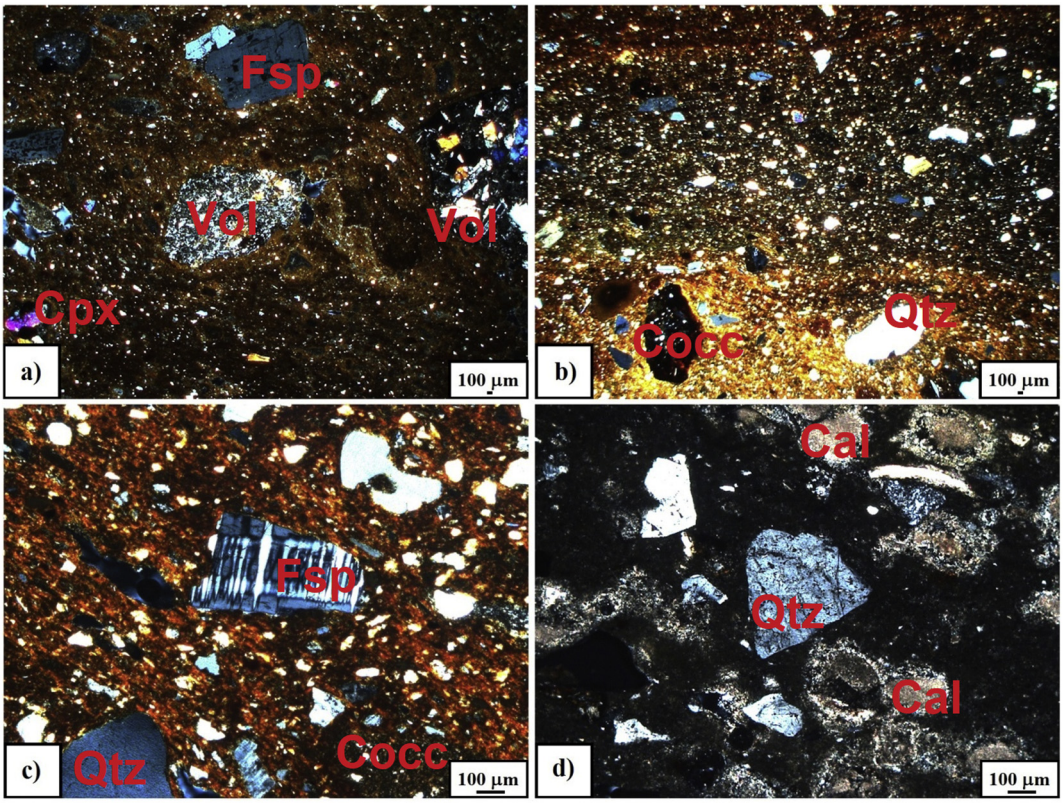

Fig. 3. Representative photomicrographs showing textural features of some pottery fragments: a) sample C1; b) sample C5; c) sample C9; d) sample C10

Table 3
Polarising optical microscopy: synthesis of data according to [29]. Amph = amphiboles; Cal = calcite; Qtz = quartz; Fsp = feldspars; Pl = plagioclase; Mic = micas; Fe-ox = iron oxides; Px = pyroxene; Car = carbonatic rocks; Met = metamorphic rocks; Vol = volcanic rocks; Cocc = cocciopesto; He = heterogeneous; Ho = homogeneous; S = sorted; M = moderately; P = poor; PS = poorly sorted; WS = well sorted; c/f/v ratio (%): coarse fraction/fine fraction/vughs = groundmass/aggregate/pore ratio. MC/1 = Type Medium-Coarse grained/Group 1; F/2 = Type Fine grained/Group 2; MF/3 = Type Medium-Fine grained/Group 3. Note: as for the c/f/v ratio (%), the semi-quantitative estimation was carried out by visual valuation, and always following [33].

Sample	Type/Group	Groundmass	Predominant inclusions	Other inclusions	Size of inclusions Min-max (μm)	Rock fragments	Size of rock fragments Min-max (μm)	Sorting	Common grain shape	c/f/v ratio (%)
C1	MC/1	He	Qtz	Pl, Fsp, Px, Mic, Fe-ox, Cal	50–1900	Vol	1000–5500	M to P	medium-low sphericity, sub-angular rounding	60/35/5
C2	F/2	Ho	Qtz	Fds, Fe-ox, Cal	50–600	Met	200–800	S to WS	medium-low sphericity, from sub-angular to rounded	45/40/15
C3	MF/3	Ho	Qtz	Pl, Fsp, Px, Mic, Amph, Fe-ox, Cal	100–800	Met, Vol, Car	200–700	S to M	medium-high sphericity, from sub-angular to rounded	45/40/15
C4	MF/3	Ho	Qtz	Pl, Fsp, Px, Mic, Amph, Fe-ox, Cal	100–900	Met, Vol, Car	200–1200	S to M	medium-high sphericity, from sub-angular to rounded	45/40/15
C5	MC/1	He	Qtz	Fsp, Pl, Mic, Fe-ox, Cal	50–2500		1000–2500	PS	medium-low sphericity, from sub-angular to sub-rounded	50/40/10
C6	F/2	Ho	Qtz	Pl, Mic, Fe-ox, Cal	50–350	Met, Car	200–600	S to WS	medium-low sphericity, from angular to sub-rounded	50/45/5
C7	F/2	Ho	Qtz	Mic, Fsp, Fe-ox	30–750	Met, Cocc	250–700	S to M	medium-low sphericity, from angular to sub-rounded	50/40/10
C8	F/2	Ho	Qtz	Mic, Fsp, Fe-ox, Cal	30–350	Met	500–1100	S to M	medium-high sphericity, from sub-angular to rounded	45/50/5
C9	MC/1	He	Qtz	Fsp, Pl, Mic, Fe-ox, Cal	50–1000	Met	400–1500	M to P	medium-low sphericity, from angular to sub-rounded	45/40/15
C10	F/2	He	Qtz	Cal, Pl, Mic, Fe-ox, Cal	50–450	Met, Car	300–600	M to P	medium-high sphericity, from sub-angular to rounded	50/40/10
C11	F/2	He	Qtz	Cal, Pl, Mic, Fe-ox, Cal	50–330	Met	200–320	S to M	medium-low sphericity, from sub-angular to sub-rounded	50/45/5
C12	MC/1	He	Qtz	Qtz, Fsp, Pl, Px, Mic, Fe-ox, Cal	30–450	Met, Vol, Cocc	150–1500	PS	medium-low sphericity, from angular to sub-rounded	40/40/20
C13	F/2	He	Qtz	Fsp, Pl, Px, Mic, Fe-ox, Cal	50–700	Met, Vol, Cocc	300–800	M to P	medium-high sphericity, from sub-angular to sub-rounded	50/40/10

clearly visible on thin and stratigraphic sections, with thicknesses up to several millimetres. No mechanical and chemical boring organisms and related damage were detected. These aspects are closely associated with the permanence conditions in the marine environment, as well as to the properties of the materials.

3.3. X-ray diffraction

As regards XRD, a semi-quantitative estimation of relative abundances obtained by considering the intensity of reflection peaks (Fig. 4) is reported in Table 4. The XRD analysis revealed that quartz is the most common mineralogical phase, followed by different amounts of plagioclase, feldspars, calcite, micas, pyroxene, hematite and clay minerals. Moreover, traces of gehlenite were detected in only two samples (namely C10 and C12), whose presence is likely linked to mineralogical and structural transformations at high-T that are essentially influenced by composition of the raw clay, its grain-size distribution, kiln temperature, and kiln atmosphere (oxidizing or reducing).

Salts like halite (sodium chloride) [34] was also detected, although in traces. It is one of the main salts that might precipitate in the seawater and be absorbed by the sherds during the permanence in the underwater environment. In samples C3, C5, C8 and C11 traces of natrojarosite ($NaFe_3(SO_4)_2(OH)_6$) were also identified. The presence of both halite and sulphate salts is relatively frequent on artefacts from shipwrecks, especially in non-desalinated samples [8].

Table 4
Semi-quantitative estimation of mineralogical phases constituting the archaeological samples and range of porosity (%). Notes: Cpx = clinopyroxene, Cal = calcite, Fsp = feldspar (group), Hem = hematite, Ill = Illite, Ms. = muscovite, Pl = plagioclase, Hl = Halite; Gh = Gehlenite; NJ = natrojarosite, xxxx = very abundant, xxx = abundant, xx = medium, x = scarce, tr = traces, – = not present; MC/1 = Type Medium-Coarse grained/Group 1; F/2 = Type Fine grained/Group 2; MF/3 = Type Medium-Fine grained/Group 3.

Sample	Type/Group	Qtz	Fsp	Pl	Ill/Ms	Cal	Hem	Cpx	Hl	NJ	Gh
C1	MC/1	xxxx	xx	xx	x	xx	x	x	–	–	–
C2	F/2	xxxx	x	x	–	–	x	–	tr	–	–
C3	MF/3	xxxx	xx	xx	x	–	x	x	–	tr	–
C4	MF/3	xxxx	xx	xx	x	–	x	x	–	–	–
C5	MC/1	xxxx	xx	xx	x	–	–	–	tr	tr	–
C6	F/2	xxxx	–	xx	–	xx	x	–	–	–	–
C7	F/2	xxxx	–	x	–	–	x	–	–	–	–
C8	F/2	xxxx	x	–	x	–	x	–	tr	tr	–
C9	MC/1	xxxx	xx	xx	–	–	x	–	tr	–	–
C10	F/2	xxxx	–	xx	–	xx	x	x	–	–	tr
C11	F/2	xxxx	–	xx	xx	x	x	–	tr	tr	–
C12	MC/1	xxx	xxx	xxx	xx	xx	x	xx	tr	–	tr
C13	F/2	xxxx	xxx	xx	x	x	x	x	–	–	–

3.4. Mechanical and chemical cleaning procedures

For cleaning procedures, samples were divided into two areas (M and C), respectively for the mechanical and chemical cleaning trials. For the first one, an ultrasonic piezoelectric device was used at frequencies between 9000 and 15,000 rpm (Fig. 5a, b). The bit was gently applied to the encrustation, which was delicately removed in order to preserve the underlying material. The sample was then carefully washed. For the second one, EDTA disodium salt was used at 5% in aqueous solution. Cellulose pulp was first soaked in the solution and then applied to the pottery surfaces (Fig. 5c, d). After 24 h, encrustations were removed from the surface by washing samples in deionised water and by using soft and hard bristle brushes, to check the effectiveness of the cleaning procedure. In some cases, it was necessary to repeat the procedure.

3.5. Chromatic and ultrasound pulse velocity measurement tests, before and after cleaning procedures

The assessment of the effectiveness of cleaning treatments is based on achieving the original appearance of the treated parts. One of the parameters that allows to measure this efficiency is to determine the chromatic changes of the pieces, comparing the appearance before and after cleaning. On each sample pertaining to the three typologies of ceramics previously identified by optical microscopy (MC – Group 1, F – Group 2 and MF – Group 3), a total of 10 measurements were performed both before and after the cleaning procedure. Table 5 shows the average

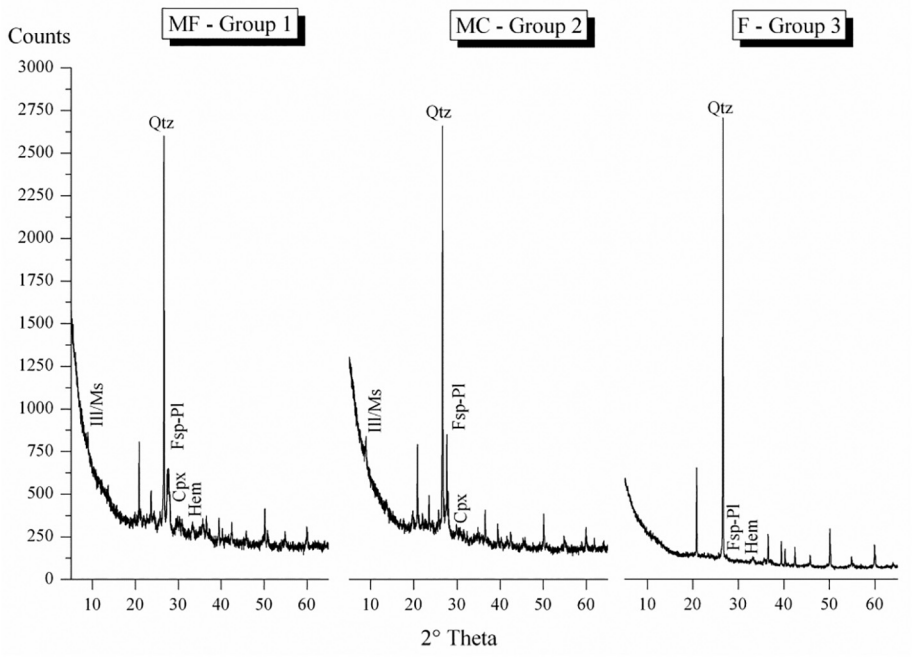

Fig. 4. Representative XRD spectra of ceramics identified by optical microscopy: MF = Medium-Fine pottery (sample C4); MC = Medium-Coarse pottery (sample C5); F = Fine pottery (sample C7).

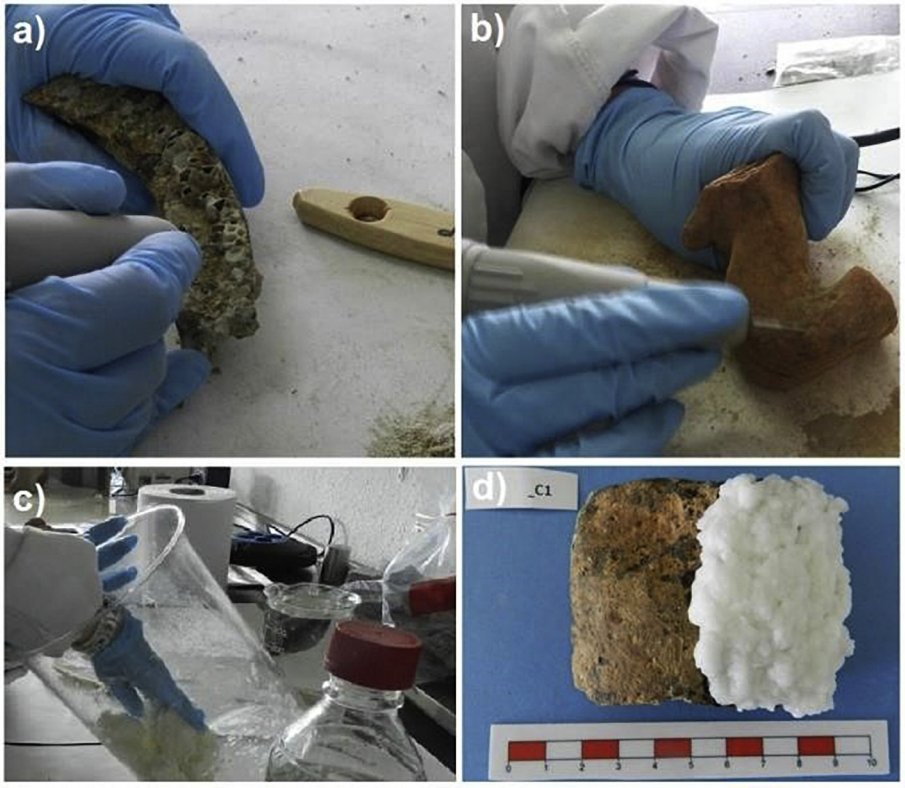

Fig. 5. Representative images of the mechanical (a; b) and chemical (c; d) cleaning.

values of the chromatic parameters before and after the cleaning procedure applied to the above-mentioned petrographic groups. Type MC and MF ceramics (i.e. Groups 1 & 3) are the ones with the greatest dispersion of chromatic data, which indicates a more heterogeneous fouling, while in those of type F chromatic variations are smaller. These ceramics belonging to type F (i.e. Group 2) have a lighter luminity (L*) and a lower chroma (C*) tending to less yellowish tones (lower b* value) than the other two types of ceramics. Both cleaning methods homogenize the chromatic results obtained in the three petrographic groups with similar chromatic values and less dispersion of the parameters. Mechanical cleaning further decreases the luminosity (L*) and chroma (C*) with respect to the samples before cleaning while in the portion subjected to chemical cleaning, the chromatic variations are smaller, being more similar to the ceramic ones before the cleaning.

Table 5
Average values of the chromatic parameters (L*, a*, b*, C*) before and after the cleaning procedure of the three typologies of ceramics (i.e. MC – Group 1; F – Group 2 and MF – Group 3). Notes: MC: Medium-Coarse pottery; MF: Medium-Fine pottery; F: Fine pottery; W: the whole area of the sample devoted to measurements before cleaning; M: Area of the sample devoted to measurements after mechanical cleaning; C: Area of the sample devoted to measurements after chemical cleaning.

	Chromatic parameters on W area, before cleaning			
Type	L*	a*	b*	C*
MC – Group 1	46.07 ± 7.25	10.54 ± 7.52	19.11 ± 7.90	22.06 ± 10.41
F – Group 2	51.06 ± 4.47	10.28 ± 3.12	15.92 ± 0.71	19.04 ± 2.27
MF – Group 3	47.69 ± 6.9	15.19 ± 5.41	20.95 ± 4.05	26.14 ± 5.65
	Chromatic parameters on M area, after Mechanical cleaning			
Type	L*	a*	b*	C*
MC – Group 1	43.98 ± 3.75	10.11 ± 4.99	18.32 ± 6.58	20.99 ± 8.07
F – Group 2	43.29 ± 1.81	12.65 ± 2.26	17.23 ± 1.80	21.40 ± 2.79
MF – Group 3	44.89 ± 8.94	11.19 ± 4.73	18.77 ± 5.45	22.09 ± 6.28
	Chromatic parameters on C area, after Chemical cleaning			
Type	L*	a*	b*	C*
MC – Group 1	47.31 ± 3.99	11.93 ± 3.63	21.55 ± 6.00	24.67 ± 6.91
F – Group 2	46.41 ± 0.18	14.98 ± 1.88	18.94 ± 1.90	24.16 ± 2.66
MF – Group 3	47.13 ± 8.18	15.19 ± 5.68	22.17 ± 4.90	27.18 ± 6.19

In Fig. 6a colour changes of each cleaning system are shown compared to the colour before cleaning in terms of ΔE*. The efficiency will be greater the more the colour of the pieces is far from the origin of the coordinates after cleaning. Mechanical cleaning is more effective since ΔE* is poorly elevated for all parts than with chemical cleaning, which is mainly due to a greater decrease in the luminosity of colour with mechanical cleaning. In general, the ceramics with a thin layer formed by algae and bryozoans and having sediment fouling are those that achieve a better degree of cleanliness. The composition of the ceramics does not seem to influence the degree of cleanliness, while porosity could play an important role, as some authors indicate, in the process of biodeterioration of materials [35]. In Fig. 6b it can be seen that the samples with lower porosity, less than 10% (i.e. C1, C6, C8, C11), are those in which mechanical cleaning achieves a greater colour change than chemical ones. Samples with a porosity between 15 and 10% (i.e. C5, C7, C10, C13), generally show similar chromatic changes, while in the one with the highest porosity (i.e. C2, C3, C4, C9, C12) the biggest colour change is achieved with chemical cleaning. This may be related to the fact that the mechanical cleaning is more superficial since it is not possible to eliminate endolithic microorganisms located in the porous ceramic system. This relationship between the porosity and the chromatic change achieved with the different cleaning techniques is defined by the regression lines with coefficients of 0.94 for ceramics with porosity close to 5% (i.e. C1, C6, C8, C11), of 0.99 for ceramics with 10% porosities (i.e. C5, C7, C10, C13) and 0.88 for those with porosities greater than 15% (i.e. C2, C3, C4, C9, C12).

As for the ultrasonic investigations, the three types of ceramic classes according to their grain size predominance (i.e. MC, F, MF) show different ultrasonic propagation velocity values (Table 6).

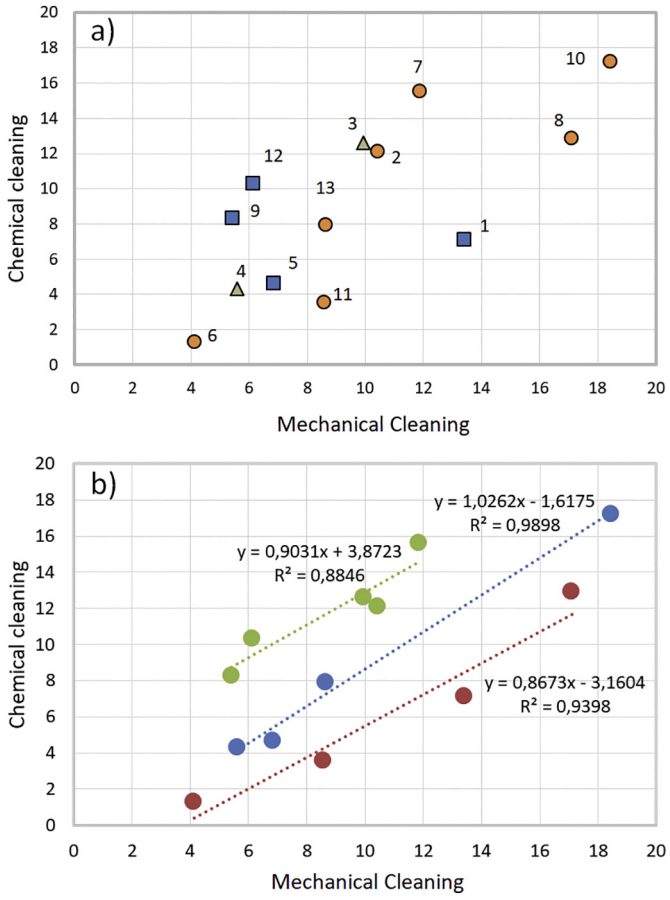

Fig. 6. Colour change (ΔE*) before and after cleaning: a) Type MC – Group 1: Blue squares; Type F – Group 2: Grey triangles; Type MF – Group 3: orange circles; b) Correlation lines based on the porosity of the ceramics. Green circles: ceramic with porosities ≥15%. Blue Circles: Ceramics with porosities of 10% and Red circles: ceramics with porosity of 5%. (For interpretation of the references to colour in this figure legend, the reader is referred to the web version of this article.)

In more detail, in direct measurements, the thicker-textured ceramics (i.e. type MC) show the highest average propagation velocity (3165 ± 667 m/s); while type MF ceramics, that are those with medium texture, show the lowest average propagation speeds with an average value of 1890 ± 67 m/s. Lastly, the finest textured ceramics (i.e. type F) display intermediate average UPV values of 2499 ± 1311 m/s, showing a greater dispersion in the measurements.

As for the results obtained by means of the indirect technique (Table 6), data show that ultrasonic velocity is higher in fine-grained ceramics than in coarse and medium-grained, maintaining a high dispersion of the measured velocities (3408 ± 1204 m/s); while in coarse-medium and medium-fine textured samples, the ultrasonic velocities are, respectively, of about 2946 ± 872 m/s and 2665 ± 182 m/s.

More specifically, in Table 7 it is shown that in the M and C areas in which samples were divided for cleaning, the speeds detected before and after cleaning are very different. This is clearly due to the presence of marine organisms, calcareous encrustations and various deposits. In particular, the samples C1 and C8 that are those with a similar superficial degree of colonization, after cleaning show that ultrasound velocity values are variable according to the cleaning method used (Table 7 and Fig. 7). Such a result suggests that, in this case, the texture of the ceramic does not influence the increase or decrease of the UPV values.

Also, samples C12 and C13 showing different degrees of colonization due to various types of marine organisms, exhibit a greater increase in UPV. Samples C6, C8, C10 and C11, belonging to Type F, are those that decrease their speed of propagation after mechanical cleaning. Therefore, the mechanical cleaning determines a deterioration of such samples' surface, while the chemical cleaning determines an increase in the UPV in the same samples, being the samples with the lowest porosity so that the presence of rooted microorganisms is lower allowing a better elimination of crusting. Samples C9 and C5 show no significant changes in their cohesion when performing chemical cleaning. These artefacts belong to the medium-textured (Type MC - Group 1) petrographic groups. The same is true for the fine-textured C10 piece (Type F - Group 2), although it undergoes major changes with mechanical cleaning. Texture ceramics Type F – Group 2 (i.e. C3 and C4) show the least changes in UPV after cleaning.

The probabilistic distribution of the 130 indirect readings of UPV before cleaning shows two populations differentiated by the change in the slope of each of them (Fig. 8a).

The first slope shows UPV values ranging from 1500 to 3000 m/s; while the second displays values greater than 3000 m/s. The population with the lowest values corresponds mainly to ceramics with fine texture (i.e. Type F – Group 2 and especially samples C11 and C13) and medium-fine (i.e. Type MF – Group 3 and especially samples C3 and C4). Conversely, among Type MC ceramics (Group 1), only sample C12 falls within this low UPV section, probably due to its high porosity

Table 6
Ultrasonic pulse velocity (m/s) before and after the cleaning procedure of the three typologies of ceramics. Notes: MC: Medium-Coarse pottery; MF: Medium-Fine pottery; F: Fine pottery; W: the whole area of the sample devoted to measurements before cleaning; M: Measures where mechanical cleaning will be carried out C: Measures where chemical-mechanical cleaning will be carried; —–: Absence of recording because the thickness of the piece is insufficient to be representative.

	Sample	UPV directy (m/s)			UPV indirecty (m/s)		
		W	M	C	W	M	C
Type MC – Group 1	C1	3834 ± 211	3685 ± 94	2673 ± 888	2673 ± 888	2618 ± 600	2689 ± 1166
	C5	2871 ± 1075	2525 ± 687	3666 ± 456	3082 ± 575	3766 ± 230	3613 ± 306
	C9	2373 ± 271	2475 ± 319	3613 ± 512	2536 ± 277	2999 ± 602	3134 ± 150
	C12	3583 ± 1514	3333 ± 1257	1832 ± 305	2793 ± 332	3601 ± 377	2918 ± 281
	Average	3165 ± 667	3004 ± 600	3311 ± 803	2946 ± 872	3246 ± 533	3088 ± 394
Type F – Group 2	C2	–	–	3082 ± 575	3666 ± 456	3060 ± 161	2306 ± 97
	C6	2837 ± 582	2944 ± 848	5140 ± 1049	5140 ± 1049	3436 ± 536	5360 ± 235
	C7	4654 ± 582	5035 ± 363	3860 ± 1026	3860 ± 1026	5311 ± 528	2016 ± 61
	C8	1822 ± 649	2151 ± 626	4140 ± 1316	4140 ± 1316	4133 ± 315	4066 ± 385
	C10	–	–	3836 ± 1292	3613 ± 512	2291 ± 29	2551 ± 371
	C11	1555 ± 483	1577 ± 325	1651 ± 83	3836 ± 1292	1205 ± 155	1261 ± 586
	C13	1625 ± 142	1451 ± 111	2150 ± 202	1651 ± 83	3827 ± 155	3816 ± 268
	Average	2499 ± 1311	2632 ± 1467	2339 ± 1272	3408 ± 1204	3367 ± 1443	3178 ± 1508
Type MF – Group 3	C3	1842 ± 769	1523 ± 199	2536 ± 277	1832 ± 305	2065 ± 151	2248 ± 217
	C4	1937 ± 210	1848 ± 236	2793 ± 332	2150 ± 202	2636 ± 124	2602 ± 131
	Average	1890 ± 67	1686 ± 230	2093 ± 95	2665 ± 182	2350 ± 404	2425 ± 250

Table 7
Mean values and standard deviation of indirect UPV (m/s) measured on ceramic samples before and after mechanical and chemical cleaning along with variation (%) among the two cleaning methods used.

Sample	Type/Group	Mechanical Cleaning		Chemical Cleaning		% Variation	
		Before	*After*	*Before*	*After*	*Mechanical*	*Chemical*
C1	MC/1	2182 ± 180	2618 ± 600	3163 ± 1067	2689 ± 1166	20.0	−15.0
C2	F/2	2545 ± 94	3060 ± 161	3620 ± 117	2306 ± 97	20.2	−36.3
C3	MF/3	2374 ± 234	2065 ± 151	2697 ± 228	2248 ± 217	−13.0	−16.6
C4	MF/3	2547 ± 78	2636 ± 124	3040 ± 300	2602 ± 131	3.5	−14.4
C5	MC/1	3704 ± 490	3766 ± 230	3627 ± 473	3613 ± 306	1.7	−0.4
C6	F/2	5960 ± 407	3436 ± 536	4320 ± 665	5360 ± 235	−42.3	24.1
C7	F/2	4570 ± 1026	5311 ± 528	2972 ± 944	2016 ± 61	16.2	−32.2
C8	F/2	5284 ± 754	4133 ± 315	2996 ± 230	4066 ± 385	−21.8	35.7
C9	MC/1	4098 ± 33	2999 ± 602	3129 ± 30	3134 ± 150	−26.8	0.2
C10	F/2	5060 ± 50	2291 ± 29	2612 ± 91	2551 ± 371	−54.7	−2.3
C11	F/2	1720 ± 40	1205 ± 155	1883 ± 47	1261 ± 586	−29.9	−20.3
C12	MC/1	1621 ± 56	3601 ± 377	2042 ± 308	2918 ± 281	122.1	42.9
C13	F/2	2347 ± 58	3827 ± 155	1952 ± 90	3816 ± 268	63.1	95.5

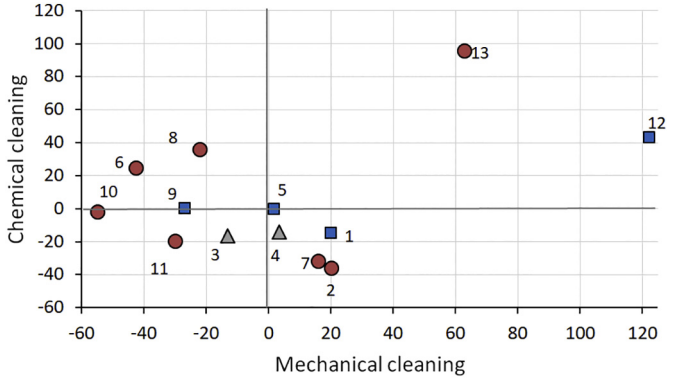

Fig. 7. % UPV variation (indirect mode) among mechanical and chemical cleaning. Type MC – Group 1: Blue squares; Type F – Group: Grey triangles; Type MF – Group 3: red circles.

(≈20%). After mechanical cleaning, the UPV increases, with a population between 1900 and 3500 m/s (Fig. 8b), where the previous ceramics (C13, C3, C4 and C12) are found except for C11, which shows lower values than before cleaning. The same occurs with chemical cleaning, where UPV values are lower than those obtained with mechanical cleaning, defining a first population ranging from 1700 to 2600 m/s. Sample C11 is subject to loss of consistency after both cleaning methods, especially when values close to 2000 and 1000 m/s were detected (Table 6). Also, sample C11 along with C12 exhibited the lowest UPV before cleaning, with values close to 2000 m/s. However, in this case, the cleaning procedures improved the UPV, showing an average value of 3733 ± 340 m/s for mechanical cleaning, and 2918 ± 280 m/s for the chemical one. As for sample C12, (Type MC – Group 1) with a porosity of 20% and a high degree of colonization of barnacles and serpulids that decreased UPV values. On the contrary, C11, with a fine texture (Type F – Group 2), and very low porosity of (5%) shows a scarce degree of algal colonization. The removal of biological encrustation surely allowed to show the original consistency of the sample. Type F ceramic

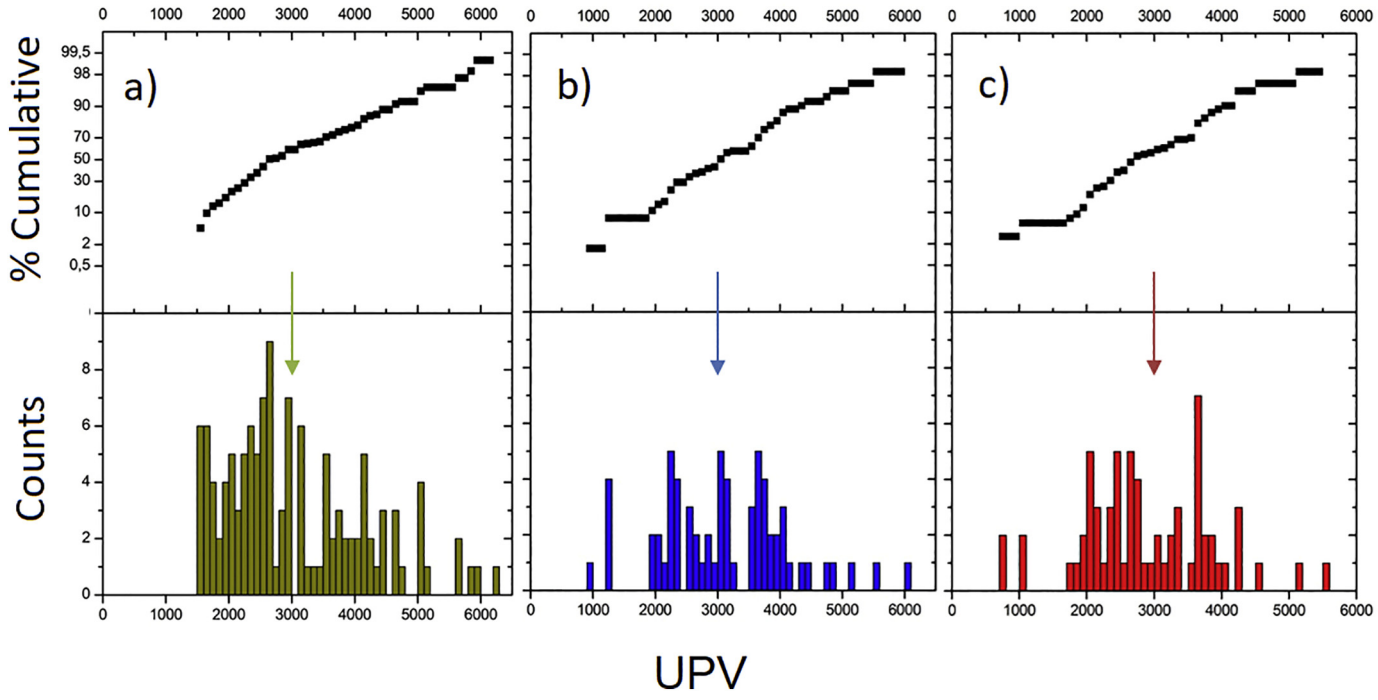

Fig. 8. Probabilistic distribution of the indirect ultrasound pulse velocity. a) Before cleaning b) after mechanical cleaning c) after chemical cleaning. Arrow: population change.

samples (Group 2) are that with the highest consistency before cleaning, with indirect UPV values greater than 4500 m/s (samples C6, C7, C8 and C10) visible in the second section or population of Fig. 8c. These samples, before cleaning, showed an intense colonization of encrusting organisms such as serpulids, bryozoa and barnacles. After mechanical cleaning, sample C7 displays the highest UPV values while all the others show lower values. Otherwise, concerning the chemical cleaning, only C6 shows the highest UPV values, while all the others show decreasing values.

4. Conclusions

This study focuses on a multidisciplinary research of archaeological pottery from underwater excavations addressed to a deep comprehension of their degradation phenomena and to test different types of cleaning in order to verify changes in the petrophysical properties of the ceramic's materials.

The main purpose is to establish proper conservation procedures based on the properties of materials and decay agents and to enhance a suitable preservation of such archaeological items to be exposed in museum exhibitions.

The mechanical and chemical cleaning procedures carried out on archaeological samples from underwater environment, with important biological growth (algae, serpulids, bryozoans, etc.) and deposits, show how the composition and texture of the ceramics do not influence the final cleaning result.

Rather, the effectiveness of cleaning is influenced by the thickness and consistency of the calcareous layers and deposits, and of the type of colonizing organisms, since the parts occupied by algae and bryozoans are easier to eliminate than those by serpulids and barnacles.

The porosity of pottery is another factor that affects the effectiveness of cleaning. In samples with low porosity, usually, mechanical cleaning is more effective, while in samples with high porosity, chemical cleaning provides better results by facilitating a deeper cleaning.

Lastly, the cleaning procedure can change the consistency of the pieces. In fact, the surface sections colonized by algae usually undergo minor changes in UPV values after cleaning because they are easier to remove.

As for ultrasound measurements, samples covered by algae and not by more encrusting species display minor changes in the ultrasound velocity after cleaning; this is probably due to the ease of algae removal compared to other more encrusting organisms.

Based on the achieved results, this work offers a further contribution to the treatment of materials coming from marine environments. In particular, the use of various diagnostic investigations and technologies allows to set-up a new protocol for the preservation of the ceramic assets before their exposure in the museum exhibitions.

CRediT authorship contribution statement

Michela Ricca: Formal analysis, Investigation, Writing - original draft, Writing - review & editing. **Beatriz Cámara:** Investigation. **Rafael Fort:** Investigation, Writing - original draft. **Mónica Álvarez de Buergo:** Investigation, Writing - review & editing. **Luciana Randazzo:** Investigation, Writing - original draft. **Mauro Francesco La Russa:** Conceptualization, Supervision, Funding acquisition.

Declaration of Competing Interest

The authors declare that they have no known competing financial interests or personal relationships that could have appeared to influence the work reported in this paper.

Acknowledgement

This work was supported by: a) PON “Ricerca e Innovazione” 2014-2020 – Fondo sociale europeo, Azione 1.2 “Mobilità dei Ricercatori” (AIM “Attraction and International Mobility” - LINEA 1), codice attività AIM1829227-3, CUP H24I19000400005, Codice ateneo DIBEST_1_R1; b) the project TOP Heritage (P2018/NMT-4372) of the Community of Madrid.

The authors wish to acknowledge the professional support of the Interdisciplinary Thematic Platform from CSIC, Open Heritage: Research and Society (PTI-PAIS).

References

[1] A. Bowen, Underwater Archaeology: The NAS Guide to Principles and Practice, second ed. Blackwell Publishing, Portsmounth, 2009.
[2] C.M. Belfiore, M.F. La Russa, L. Randazzo, G. Montana, A. Pezzino, S.A. Ruffolo, P. Aloise, Laboratory tests addressed to realize customized restoration procedures of underwater archaeological ceramic finds, Appl. Phys. A-Mater. 114 (2014) 741–752.
[3] S. Guirado, F.J. Fortes, J. Javier Laserna elemental analysis of materials in an underwater archeological shipwreck using a novel remote laser-induced breakdown spectroscopy system, Talanta 137 (2015) 182–188.
[4] N. Rovella, V. Comite, M. Ricca, The methodology of investigation on red- and black-figured pottery of unknown provenance, IJCS 7 (2016) 954–964.
[5] T. Palomar, Characterization of the alteration processes of historical glasses on the seabed, Mater. Chem. Phys. 214 (2018) 391–401.
[6] C. Pearson, in: C. Pearson (Ed.), Conservation of Marine Archaeological Objects, Butterworths, London 1987, p. 99.
[7] G.M. Crisci, M.F. La Russa, M. Macchione, M. Malagodi, A.M. Palermo, S.A. Ruffolo, Study of archaeological underwater finds: deterioration and conservation, Appl. Phys. A-Mater. 100 (2010) 855–863.
[8] P. López-Arce, A. Zornoza-Indart, L. Gomez-Villalba, E. Mercedes Pérez-Monserrat, M. Alvarez de Buergo, G. Vivar, R. Fort, Archaeological ceramic amphorae from underwater marine environments: influence of firing temperature on salt crystallization decay, J. Eur. Ceram. Soc. 33 (2013) 2031–2042.
[9] M. Wahl, Marine epibioses: fouling and antifouling: some basic aspects, Mar. Ecol. Prog. Ser. 58 (1989) 175–189.
[10] M.E. Callow, J.A. Callow, Marine biofouling: a sticky problem, Biologist 49 (2002) 1–5.
[11] E. Casoli, S. Ricci, A. Belluscio, M.F. Gravina, G. Ardizzone, Settlement and colonization of epi-endobenthic communities on calcareous substrata in an underwater archaeological site, Mar. Eco. 36 (2015) 1060–1074.
[12] P. Aloise, M. Ricca, M.F. La Russa, S.A. Ruffolo, C.M. Belfiore, G. Padeletti, G.M. Crisci, Diagnostic analysis of stone materials from underwater excavations: the case study of the Roman archaeological site of Baia (Naples, Italy), Appl. Phys. A-Mater. 114 (2014) 655–662.
[13] C.M. Belfiore, M.F. La Russa, D. Barca, G. Galli, A. Pezzino, S.A. Ruffolo, M. Viccaro, G.V. Fichera, A trace element study for the provenance attribution of ceramic artefacts: the case of Dressel 1 amphorae from a late-Republican ship, J. Archaeol. Sci. 43 (2014) 91–104.
[14] M.F. La Russa, M. Ricca, C.M. Belfiore, S.A. Ruffolo, M. Álvarez De Buergo Ballester, G.M. Crisci, The Contribution of Earth Sciences to the Preservation of Underwater Archaeological Stone Materials: an Analytical Approach, JCS 6 (2015) 335–348.
[15] M. Ricca, V. Comite, M.F. La Russa, D. Barca, Diagnostic analysis of bricks from the underwater archaeological site of Baia (Naples, Italy): preliminary results, Rend. Online Soc. Geol. It. 38 (2016) 85–88.
[16] B. Cámara, M. Álvarez de Buergo, M. Bethencourt, T. Fernández-Montblanc, M.F. La Russa, M. Ricca, R. Fort, Biodeterioration of marble in an underwater environment, Sci. Total Environ. 609 (2017) 109–122.
[17] L. Randazzo, M. Ricca, S.A. Ruffolo, M. Aquino, Davidde Petriaggi, F. Enei, M.F. La Russa, An Integrated Analytical Approach to Define the Compositional and Textural Features of Mortars Used in the Underwater Archaeological Site of Castrum Novum (Santa Marinella, Rome, Italy), Minerals 9 (2019) 268.
[18] D. Gregory, P.K. Jensen Strætkvern, Conservation and in situ preservation of wooden shipwrecks from marine environments, J. Cult. Herit. 13 (2012) 139–148.
[19] UNESCO, Convention on the Protection of the Underwater Cultural Heritage, Paris 2001.
[20] B. Davidde, Underwater archaeological parks: a new perspective and a challenge for conservation-the Italian panorama, IJNA 31 (2002) 83–88.
[21] M. Ricca, C.M. Belfiore, S.A. Ruffolo, D. Barca, M. Alvarez De Buergo, G.M. Crisci, M.F. La Russa, Multi-analytical approach applied to the provenance study of marbles used as covering slabs in the archaeological submerged site of Baia (Naples, Italy): the case of the “Villa con ingresso a protiro”, Appl. Surf. Sci. 357 (2015) 1369–1379.
[22] F. Bruno, A. Gallo, L. Barbieri, M. Muzzupappa, G. Ritacco, A. Lagudi, M.F. La Russa, S.A. Ruffolo, G.M. Crisci, M. Ricca, V. Comite, B. Davidde, G. Di Stefano, R. Guida, The CoMAS project: new materials and tools for improving the in-situ documentation, restoration and conservation of underwater archaeological remains, Mar. Technol. Soc. J. 50 (2016) 108–118.
[23] S.A. Ruffolo, M. Ricca, A. Macchia, M.F. La Russa, Antifouling coatings for underwater archaeological stone materials, Progr. Orga. Coat. 104 (2017) 64–71.

[24] H.T. Dede, M.İ.C. Taner, B. Ridolfi, A. Costanzi, R. Allotta, B. Design and testing of an innovative cleaning tool for underwater applications, P. I. Mech. Eng. M-J Eng 230 (2016) 579–590.
[25] N. Rovella, F. Bruno, B. Davidde Petriaggi, T. Makris, P. Raxis, M.F. La Russa, A usable and people-friendly cultural heritage: MAGNA project, on the route from Greece to Magna Graecia, Heritage 2 (2019) 1350–1368.
[26] J.H. D'Arms, Romans on the bay of Naples, in: F. Zevi (Ed.), Romans on the Bay of Naples and Other Essays on Roman Campania, Edipuglia, Bari, 2003.
[27] M. Ricca, M.F. La Russa, S.A. Ruffolo, B. Davidde, D. Barca, G.M. Crisci, Mosaic marble tesserae from the underwater archaeological site of Baia (Naples, Italy): determination of the provenance, Eur. J. Mineral. 26 (2014) 323–331.
[28] Normal 43/93, Misure colorimetriche di superfici opache, in: Raccomandazioni Normal: alterazioni dei materiali lapidei e trattamenti conservativi: proposte per l'unificazione dei metodi sperimentali di studio e di controllo. , Roma CNR, ICR, 1993.
[29] A. Salazar, G. Safont, L. Vergara, E. Vidal, Pattern recognition techniques for provenance classification of archaeological ceramics using ultrasounds, Pattern Recogn. Lett. 135 (2020) 441–450.
[30] A. Salazar, L. Vergara, ICA Mixtures Applied to Ultrasonic Non-destructive Classification of Archaeological Ceramics, EURASIP J. Adv. Sig. Pr. (2010) 125201, https://doi.org/10.1155/2010/125201.
[31] A. Salazar, R. Miralles, A. Parra, L. Vergara, J. Gosalbez, Ultrasonic signal processing for archaeological ceramic restoration, IEEE Publisher, ICASSP Proceedings 2006, pp. 1160–1163, https://doi.org/10.1109/ICASSP.2006.1660865 , ISBN: 1-4244-0469-X.
[32] C.N. Bianchi, La biocostruzione negli ecosistemi marini e la biologia marina italiana, Biol. Mar. Mediterr. 8 (2001) 112–130.
[33] I.K. Whitbread, Greek Transport Amphorae: A Petrological and Archaeological Study, British School at Athens, Fitch Laboratory Occasional Paper 4, Athens 1995.
[34] S. Jang, B. Nam, D. Park, H. Kim, C.H. Lee, J.E. Yu, Desalination characteristics for ceramics excavated from Taean shipwreck, Korea, J. Cul. Herit. 14 (2013) 229–237.
[35] L. Graziani, E. Quagliarini, M. D'Orazio, The role of roughness and porosity on the self-cleaning and anti-biofouling efficiency of TiO_2-cu and TiO_2-Ag nanocoatings applied on fired bricks, Constr. Build. Mater. 129 (2016) 116–124.